

# Fast fabrication of super-hydrophobic surfaces on polypropylene by replication of short-pulse laser structured molds

J. Bekesi · J.J.J. Kaakkunen · W. Michaeli · F. Klaiber ·  
M. Schoengart · J. Ihlemann · P. Simon

Received: 12 April 2010 / Accepted: 16 April 2010 / Published online: 7 May 2010  
© Springer-Verlag 2010

**Abstract** A new two-step method, facilitating the rapid generation of super-hydrophobic surface structures via parallel laser processing followed by a replica generation by injection molding is reported. A self-made fused silica-based diffractive optical element (DOE) is applied to distribute the laser energy into a  $25 \times 25$  dot matrix. This DOE is used as a transmission mask for surface ablation of metal molds, applying short-pulse UV laser pulses. In a subsequent process step, replicas of the processed stamp are produced by variothermal injection molding, enabling the mass production of the surface pattern on plastics parts. The resulting topography facilitates a super-hydrophobic behavior of the fabricated components.

## 1 Introduction

Micro- and/or nano-structured surfaces give rise to a variety of new functionalities including super-hydrophobic behavior, particular tribological properties, field amplification capability, etc., holding great potential for numerous novel

applications [1, 2]. All these applications are generating a continuously increasing demand on fast, simple, flexible and economical fabrication technologies. Laser ablation is a well-suited method for the fabrication of micron sized or even smaller surface structures on a large variety of materials. Especially the generation of small feature sizes in the micrometer range or smaller on materials of high heat conductivity might necessitate the use of special laser systems. In such cases, application of short laser pulses with picosecond pulse durations or shorter is needed [3]. Applying short-wavelength irradiation ensures a further increased spatial resolution [4].

Parallel processing techniques have clear advantages over sequential methods from the point of view of the reachable maximum processing speed, representing a key issue in most industrial applications. Focus scanning offers the capability of creating arbitrary structures with great flexibility, but with a limited processing speed. Especially for the generation of periodic structures, the application of interference- or mask projection techniques [4–7] can significantly speed up the process, creating a large number of features simultaneously, using only moderate number of pulses. However, in order to get the required energy density, which conveniently overtakes the damage threshold of the ablated material, very high pulse energies or very high overall transmittance of the optical setup is required. To scale up the energy of the laser system is usually very expensive. A more favorable way would be to reduce the losses of the beam delivery system. At this point the transmission efficiency of the applied optical elements becomes very important. Amplitude masks usually have a relatively low transmission, because the photons hitting the highly reflective parts of the mask cannot be used for the ablation process. Therefore diffractive phase masks, which do not influence the amplitude but only the phase of light, are often used for efficient mask

---

J. Bekesi (✉) · J. Ihlemann · P. Simon  
Laser-Laboratorium Göttingen e.V., Hans-Adolf-Krebs-Weg 1,  
37077 Göttingen, Germany  
e-mail: [jozsef.bekesi@llg-ev.de](mailto:jozsef.bekesi@llg-ev.de)

J.J.J. Kaakkunen  
Department of Physics and Mathematics, University of Eastern  
Finland, P.O. Box 111, 80101 Joensuu, Finland  
e-mail: [jarno.kaakkunen@uef.fi](mailto:jarno.kaakkunen@uef.fi)

W. Michaeli · F. Klaiber · M. Schoengart  
IKV Institute of Plastics Processing at RWTH Aachen University,  
Pontstraße 55, 52062 Aachen, Germany

F. Klaiber  
e-mail: [klaiber@ikv.rwth-aachen.de](mailto:klaiber@ikv.rwth-aachen.de)

illumination. The phase-shifting function of an element operating in transmission is implemented by a lateral variation of the optical path length, e.g. by variation of the geometrical thickness of the material. Such elements are commonly used for the visible and IR spectral range. Applying laser pulses in the short-wavelength range necessitates the application of mask materials with high transmission in the UV (e.g. fused silica,  $\text{CaF}_2$ ,  $\text{MgF}_2$ ). Fast, cheap, and flexible manufacturing of such optical components could also be achieved by applying conventional laser processing methods. However, particularly the low absorption of such materials makes mask fabrication by laser ablation rather complicated [8]. These difficulties can be overcome by applying a fabrication method based on UV laser backside patterning of silicon suboxide layers ( $\text{SiO}_x$ ) on fused silica substrates, and their subsequent oxidation, resulting in a UV-grade surface relief element [9–11]. The applied suboxide layer has a high absorption in the UV, making the ablation process easy. The precisely defined interface between substrate and layer allows for ablation with exact depth control, and perfect optical surface quality. Backside ablation ensures to remove the complete  $\text{SiO}_x$  layer without damaging the highly transparent  $\text{SiO}_2$  substrate, creating smooth ablated features with perfect optical quality. Also the depth control is very exact this way, necessary to generate highly efficient phase elements, because the height of the ablated features can be defined by the layer thickness.

In this paper, we propose an optical arrangement to generate a 2D array of focused spots on the sample surface by UV short-pulse laser ablation. The optical setup is based on a self-made phase-only diffractive optical element (DOE), generated on fused silica by ns backside ablation of a silicon suboxide layer at 193 nm irradiation wavelength. The designed 2-level DOE generates  $25 \times 25$  spots in the Fourier plane of the optical setup, which is imaged onto the sample surface. This setup allows the texturing of metallic molds. They can be replicated by injection molding, generating a complementary structure of that of the stamp texture on a big variety of plastic materials. Proper combination of used materials, the applied textures and the duplication circumstances allow generating super-hydrophobic surface properties. Various types of polypropylene materials have been successfully investigated, and turned into super-hydrophobic surfaces.

## 2 Mask fabrication

An Iterative Fourier Transform Algorithm (IFTA) was used to design the phase masks [12, 13]. It was a 2-level phase element, generating the desired intensity distribution on the optical axis, without any offset, in the form of a  $25 \times 25$  dot matrix. Although in this design the separation of the 0th order from the 1st order pattern is not possible, because of its

high efficiency it still can be advantageous for some particular applications. For point-symmetrical structures (like an  $N \times N$  dot matrix) the 1st order beams can be overlapped ensuring an effectively doubled efficiency compared to that of an off-axis design. Additionally, the 0th order beam is focused in the Fourier plane of the element and coincides with the central dot (if odd number of dots is applied) like in our case. The mask was designed to consist of  $367 \times 367$  pixels, with a pixel size of  $27 \mu\text{m}$ , yielding a full aperture of roughly  $10 \text{ mm} \times 10 \text{ mm}$ . For the machining of the DOE we used a commercial excimer laser delivering UV-nanosecond laser pulses at a wavelength of  $\lambda = 193 \text{ nm}$ . To generate the required phase steps, the pixels were ablated in the  $\text{SiO}_x$  layer by imaging a square aperture onto the backside of the quartz substrate. Subsequently the  $\text{SiO}_x$  layer was converted into  $\text{SiO}_2$  in an annealing process, heating the mask over 8 hours up to  $1000^\circ\text{C}$  in atmospheric ambience. During this process the  $\text{SiO}_x$  layer gets the same transparency like bulk silica, ensuring high transmission of the mask. In order to check the performance of the DOE we used femtosecond UV pulses at 248 nm wavelength [14], as later on for the generation of hole matrices. A phosphor plate was placed in the Fourier plane and illuminated by the generated dot matrix, to observe the generated intensity distribution. This pattern was imaged onto a CCD camera and was recorded with a beam analyzing software. Such an image is shown in Fig. 1a. In Fig. 1b a vertical cross section of the intensity distribution of the middle line (containing the 0th order beam) is shown, demonstrating the uniformity and the 0th order suppression of the mask. The 0th order suppression was found to be satisfactory for our application; the peak overlapping with the 0th order was around 50% higher than the average peak-height. The efficiency of the DOE was measured to be around 61%, in good agreement with the theoretically calculated value of 72%. For comparison a similar amplitude mask would have a maximal transmission of 11%.

## 3 Laser processing of metallic molds

In the experiments to machine steel molds we used a UV short-pulse laser system delivering  $\sim 1 \text{ ps}$  pulses at 248 nm [14]. The middle part of the beam was cut by an aperture of  $10 \times 10 \text{ mm}$ . The DOE generating a  $25 \times 25$  dot matrix in its Fourier plane was placed behind this aperture. A telescope system consisting of a positive ( $f = 1500 \text{ mm}$ ) and a negative ( $f = -250 \text{ mm}$ ) lens was used to adjust the effective focal length of the system and resulted in a pattern size of  $24 \times 24 \text{ mm}$  in the Fourier plane of the phase element. In the experiments we intended to drill high aspect ratio holes, necessitating a background-free illumination. In order to further reduce background radiation we used a hole-matrix aperture in the Fourier plane of the DOE, which only

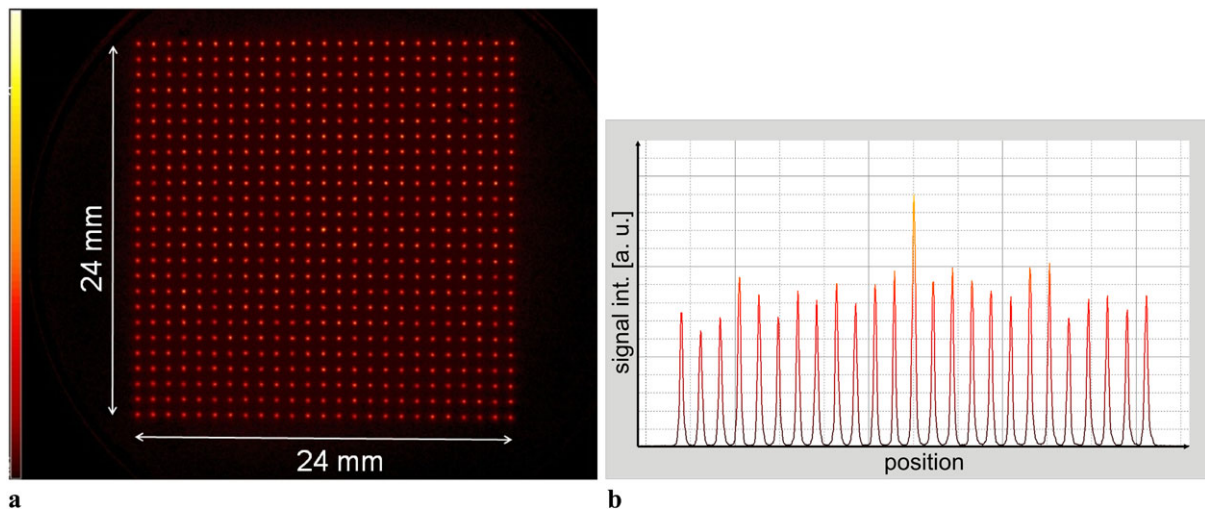
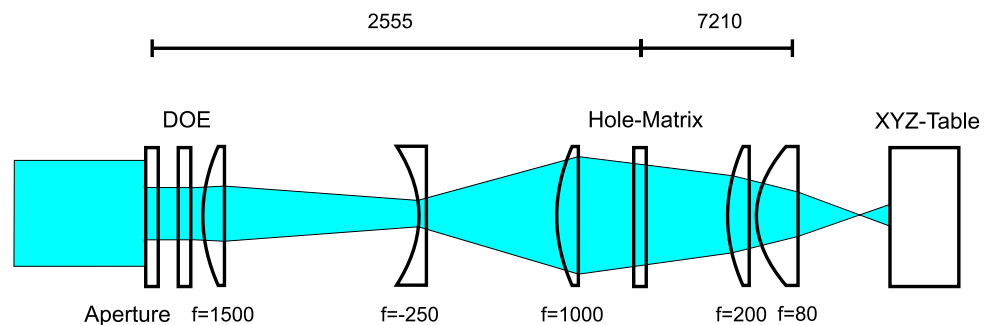


**Fig. 1** Intensity distribution generated by the DOE in the Fourier plane measured with a CCD (a) and (b) the intensity distribution across the middle horizontal line

**Fig. 2** Optical setup for generation of hole matrices



transmitted the main intensity peaks and blocked the residual radiation in between them. Furthermore, just before the Fourier plane, a field lens was applied to keep the beam size small on the imaging lenses, thus minimizing the aberrations of the imaging system. The Fourier plane was imaged with a lens system consisting of 2 lenses onto the sample surface (Fig. 2).

By changing the distance between the Fourier plane and the imaging lenses variation of the demagnification factor was possible, allowing a fairly uncomplicated way to control the size and the period of the dot matrix.

For the ablation of steel molds the generated pattern shown in Fig. 1 was imaged onto the sample surface with a demagnification factor of 75. The mold sample material was tool steel (1.2767). The size of the illuminated area was  $320 \mu\text{m} \times 320 \mu\text{m}$ , yielding a periodicity of  $\sim 13 \mu\text{m}$  with feature sizes of  $\sim 5 \mu\text{m}$ . Each matrix was illuminated by 150 pulses with 0.7 mJ energy (measured just in front of the imaging lenses). In order to reach a structured surface area large enough for further characterization the mold was illuminated by stitching the  $25 \times 25$  dot matrix fields. The applied translation stages allowed us to place them next to each other with a precision of 1–2 microns, fully satisfac-

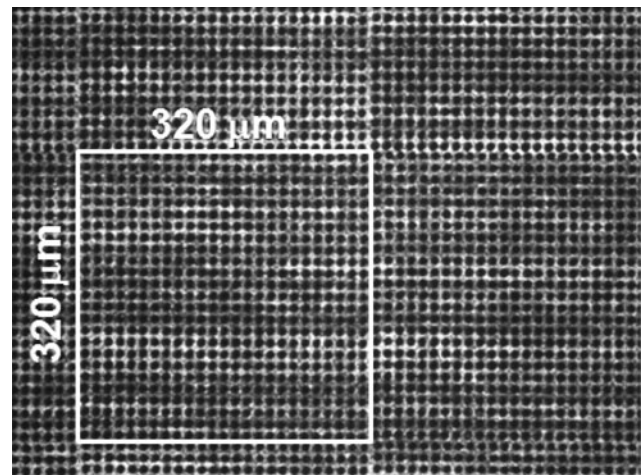


**Fig. 3** Light microscope image of a steel mold irradiated with 150 laser pulses of 0.7 mJ pulse energy. The size of the illuminated area in one process step is  $320 \times 320 \mu\text{m}^2$ , containing  $25 \times 25$  holes. The period of the structure is  $\sim 13 \mu\text{m}$ , the diameter of the holes is  $\sim 5 \mu\text{m}$

tory for our application. Such an illuminated area is shown in Fig. 3.

The light microscopic image shows a part of the irradiated area of a steel mold, structured with  $3 \mu\text{m}$  diameter



holes with a periodicity of 13  $\mu\text{m}$  in both horizontal and vertical direction. The  $25 \times 25$  hole matrix is marked with a white box, indicating the illuminated area of  $320 \times 320 \mu\text{m}^2$  machined in one step. This steel mold was replicated by injection molding on polypropylene.

#### 4 Replication by injection molding

The mold insert was mounted into a high-precision injection mold, which was designed and built particularly for the

replication of micro-structured plastics parts. In this work, a hydraulic KM CX 160-1000 injection molding machine was used. A standard polypropylene material (Sabic PP 513) commonly used for biomedical and packaging applications was chosen. The plasticizing temperature was  $200^\circ\text{C}$  with a mold temperature of  $30^\circ\text{C}$  and a maximum holding pressure of 700 bar. It has been shown that elevated mold temperatures during the injection are necessary in order to ensure a precise molding of surface structures in the  $\mu\text{m}$ -range [15]. To achieve a well defined and fast changing temperature profile, an inductive mold heating system in combination with

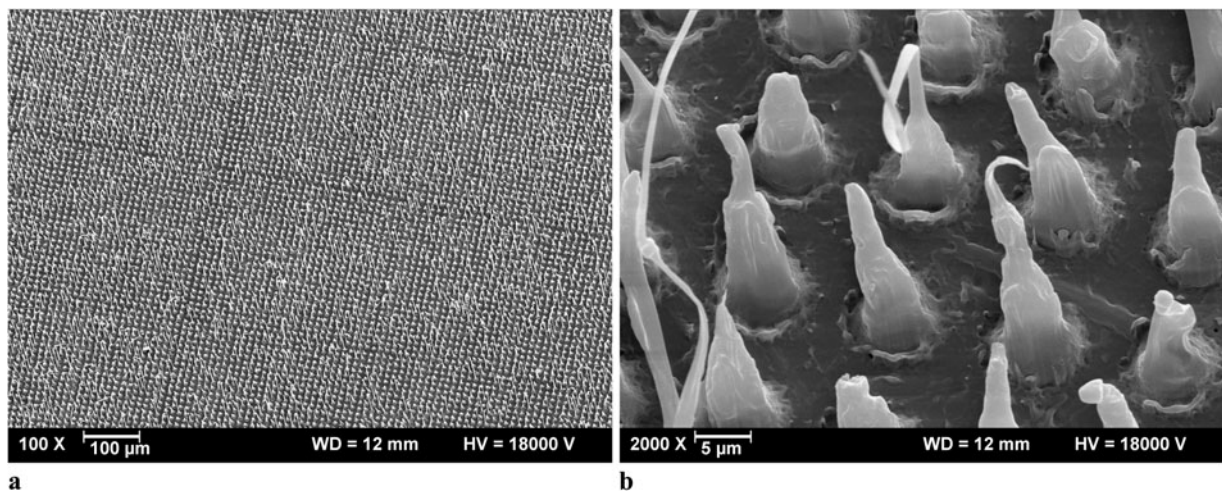


**Fig. 4** SEM pictures of a replica made of the mold shown in Fig. 3, applying variothermal injection molding. Period  $\sim 13 \mu\text{m}$ , base diameter of the pins  $\sim 5 \mu\text{m}$ , material: polypropylene. **(b)** is a close up view of **(a)**

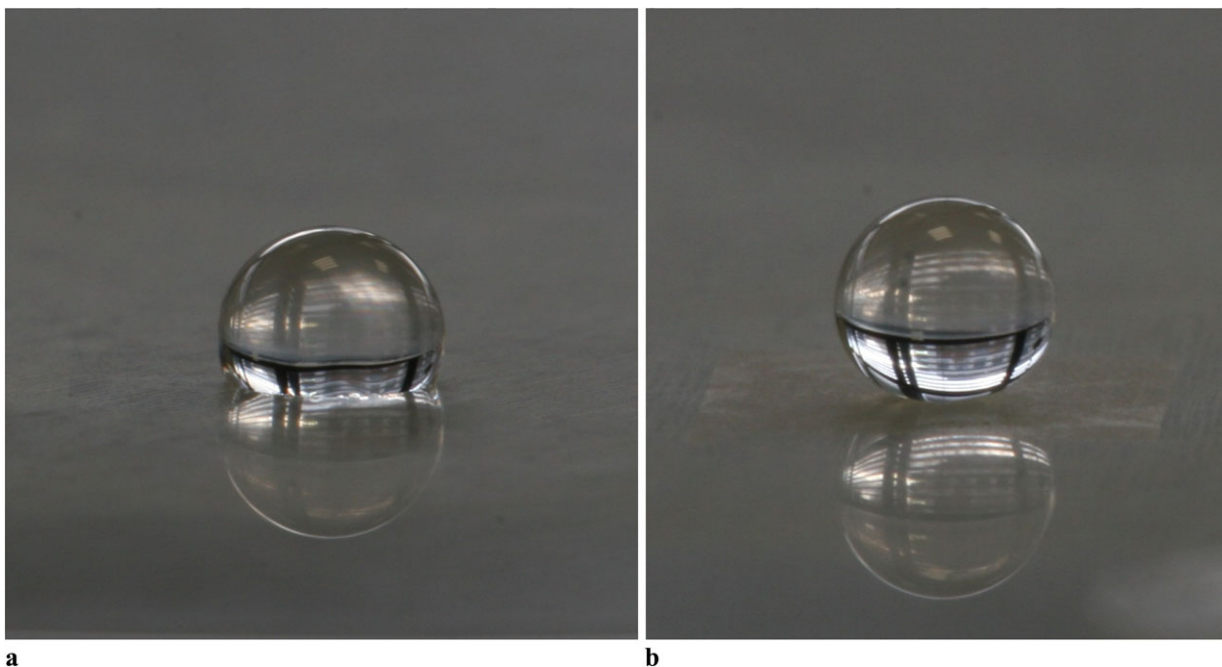


**Fig. 5** Contact angle measurement on a replicated PP sample, **(a)** without and **(b)** with surface texture

conventional mold cooling was used. This system for vario-thermal process control is composed of an inductor heating unit and a robot. The robot automatically places the inductor in front of the micro-structured cavity while the mold is open. Using a pyrometer-based temperature control, a defined heat up of the cavity wall (up to 60 K/s were measured) is achieved without destroying the fragile micro-structures by uncontrolled high temperatures. After the mold is heated up, the inductor is being moved out, the mold closes and the injection process starts.

In Fig. 4 SEM pictures of a replica on polypropylene (Sabic PP513) is shown made by the above described injection molding technique. The applied laser parameters were identical to those presented in Fig. 3. Picture (a) shows an overview of the generated periodic bump structure. Also the original irradiated fields are visible. Picture (b) shows a magnified image of the bumps, generating the hydrophobic effect.

## 5 Hydrophobicity

The replicated surfaces were investigated with respect to hydrophobicity. The results showed the possibility of rapid generation of surface structures on polypropylene with greatly increased hydrophobic properties. Figure 5 shows distilled water droplets on non-textured (a) and textured parts (b) of the sample. The contact angle measurement showed that the naturally neutral surface with contact angles of around 90 degree can be converted into super-hydrophobic surfaces with contact angles of more than 160 degrees.

**Acknowledgements** Valuable contributions of the University of Eastern Finland for the contact angle measurements are gratefully acknowledged.

Regarding the injection molding experiments the authors would like to thank the German Research Foundation DFG for the support of the depicted research within the Cluster of Excellence “Integrative Production Technology for High-Wage Countries” at RWTH Aachen University.

This work was also partly supported by TEKES, the Finnish Agency for Technology and Innovation.

## References

1. H.Y. Erbil, A.L. Demirel, Y. Avci, O. Mert, *Science* **299**, 1377 (2003)
2. B. Bushan, Y.C. Yung, *Ultramicroscopy* **107**, 1033 (2007)
3. S. Küper, M. Stuke, *Appl. Phys. B* **44**, 199 (1987)
4. J.-H. Klein-Wiele, J. Bekesi, P. Simon, *Appl. Phys. A* **79**, 775 (2004)
5. M. Campbell, D.N. Sharp, M.T. Harrison, R.G. Denning, A.J. Turberfield, *Nature* **404**, 53 (2000)
6. S. Matsuo, T. Kondo, V. Mizeikis, H. Misawa, *Proc. SPIE* **4655**, 327 (2002)
7. J. Bekesi, J. Meinertz, J. Ihlemann, P. Simon, *J. Laser Micro/Nanoeng.* **2**, 221 (2007)
8. J. Ihlemann, M. Schulz-Ruhtenberg, T. Fricke-Begemann, *J. Phys., Conf. Ser.* **59**, 206–209 (2007)
9. M. Schulz-Ruhtenberg, J. Ihlemann, J. Heber, *Appl. Surf. Sci.* **587**, 190 (2005)
10. J.-H. Klein-Wiele, J. Bekesi, P. Simon, J. Ihlemann, *J. Laser Micro/Nanoeng.* **1**, 221 (2006)
11. J. Ihlemann, *J. Optoelectron. Adv. Mater.* **7**, 1191–1195 (2005)
12. J. Bekesi, D. Schäfer, J. Ihlemann, P. Simon, *Proc. SPIE* **4977**, 235 (2003)
13. J. Turunen, F. Wyrowski, *Diffraction Optics for Industrial and Commercial Applications* (Akademie Verlag, Berlin, 1997)
14. S. Szatmari, F.P. Schäfer, *Opt. Commun.* **68**, 196 (1988)
15. W. Michaeli, F. Klaiber, S. Scholz, in *Proceedings of the Fourth International Conference on Multi-Material Micro Manufacture* (Elsevier, Amsterdam, 2008)